Magnetic Resonance in Medicine 42:704–713 (1999)

Nonsubtractive Spiral Phase Contrast Velocity Imaging

Lai-Chee Man,* John M. Pauly, Dwight G. Nishimura, and Albert Macovski

Phase contrast velocity imaging is a standard method for accurate in vivo flow measurement. One drawback, however, is that it lengthens the scan time (or reduces the achievable temporal resolution) because one has to acquire two or more images with different flow sensitivities and subtract their phases to produce the final velocity image. Without this step, non-flow-related phase variations will give rise to an erroneous, spatially varying background velocity. In this paper, we introduce a novel phase contrast velocity imaging technique that requires the acquisition of only a single image. The idea is to estimate the background phase variation from the flow-encoded image itself and then have it removed, leaving only the flow-related phase to generate a corrected flow image. This technique is sensitive to flow in one direction and requires 50% less scan time than conventional phase contrast velocity imaging. Phantom and in vivo results were obtained and compared with those of the conventional method, demonstrating the new method's effectiveness in measuring flow in various vessels of the body. Magn Reson Med 42:704–713, 1999. © **1999 Wiley-Liss, Inc.**

Key words: MRI; phase contrast; flow; phase estimation

Phase contrast (PC) velocity imaging has become a widespread method for both qualitative and quantitative assessments of flow since its first report (1). In standard PC velocity imaging, one image is acquired per flow dimension, and one more image is acquired as a reference for the removal of non-flow-related background phase, which otherwise would appear as artifacts in the final flow image. As a result, a minimum of two images are acquired to produce the velocity image. This represents a significant penalty in scan time (or temporal resolution in the case of dynamic imaging), compromising its utility in highly time-constrained situations such as breath-hold imaging, real-time imaging, and 3D imaging in general. Motivated by the need to shorten the scan time of PC velocity imaging, we propose a method that requires the acquisition of a single flow-encoded image from which both anatomical and flow information are derived. In this method, non-flow-related incidental background phase is estimated from the flow-encoded image itself instead of from a separately acquired reference image. Because only one flow-encoded image is acquired, our method is sensitive to flow in a single dimension, which is sufficient for many applications.

In this paper, the proposed method is combined with spiral readout trajectories to achieve short imaging times. Spiral imaging (3,4) makes use of oscillating readout gradients to produce fast coverage of k-space. Spirals inherently have good flow properties (4,5) and therefore are ideal for imaging fast flow. Their use in conventional PC velocity imaging has been reported (6,7).

BACKGROUND

Conventional PC Velocity Imaging

It is well-known that under the influence of a magnetic field gradient, moving spins acquire a phase different from that of stationary spins. In MRI, the phase (ϕ) of an image voxel due to flow is proportional to its flow velocity (v) when subjected to a gradient waveform of zero total area (2):

$$\phi = \gamma M_1 v. \qquad [1]$$

In Eq. [1], M_1 is the first moment of the gradient waveform evaluated at the echo (center of k-space). This ignores the effects of acceleration and other higher order motions, which usually are quite small. The quantity $\pi/(\gamma M_1)$, which we shall denote by v_M, represents the highest flow velocity (both forward and backward) an experiment can measure without phase wrap-around, which produces ambiguities.

In addition to the above-mentioned phase due to flow, an MR image generally includes some undesirable background phase. Contributing sources include off-resonance and susceptibility effects, imperfect timing, radiofrequency (RF) nonlinearity, spatially varying receiver coil responses, gradient Maxwell terms (8), and eddy currents, among others. If uncorrected, this incidental phase will give an erroneous background velocity to the PC velocity image. Early researchers chose to ignore this error, which was relatively small for their spin-echo images, but most researchers later recognized the importance of correcting for the incidental phase errors to reduce image artifacts and measurement errors (2,9,10). Correction is particularly important in the prevalent methods of flow imaging, which avoid the use of spin echoes because of low vessel signals. Currently, standard PC imaging solves this problem by acquiring an additional image in which only the flow-encoding gradient is changed. A phase subtraction of the two images will therefore leave only the flow-induced phase non-zero. The remaining error due to different eddy currents for the two sequences can be corrected (11–13).

Shortening Scan Time

Acquiring an additional phase reference image requires more scan time. Attempts to reduce scan time have been reported. Jhooti et al. (14) replaced the high-resolution reference scan with a low-resolution one to save time. Using 32 phase encoding steps for the reference instead of the 128 steps for the high-resolution flow-encoded image, the mean flow rate had a moderate 22% error with respect

Magnetic Resonance Systems Research Laboratory, Department of Electrical Engineering, Stanford University, Stanford, California.

Grant sponsor: National Institutes of Health; Grant numbers: CA-50948; HL-39297; Grant sponsor: GE Medical Systems.

*Correspondence to: Lai-Chee Man, Ph.D., 303 Durand Building, Department of Electrical Engineering, Stanford University, Stanford, CA 94305-4055. E-mail: lcman@isl.stanford.edu

Received 10 July 1998; revised 7 June 1999; accepted 8 June 1999.

to conventional PC velocity imaging. Another way to shorten the scan time in time-resolved images was proposed by Jhooti et al. (15). Using an idea similar to keyhole imaging (16), they updated the central region of k-space at the time resolution desired and updated the outer regions of k-space at a slower rate, thus reducing the total number of phase encode views acquired. Using only 50% of the conventional number of phase encodes, they reported a very good 3% volume flow rate error. However, ringing artifacts in both the magnitude and PC images were also noticed.

In the next section, we describe an alternative method to obtain a reliable PC velocity image from a single flow-encoded image. This represents a 50% reduction of scan time and is applicable to both time-resolved and non-time-resolved imaging. It also gives an artifact-free magnitude image in most circumstances.

MATERIALS AND METHODS

Nonsubtractive PC Imaging

It has been observed that the background phase associated with an MR image often contains low spatial frequency (17,18). This in fact has been exploited in noise reduction (19,20), partial k-space reconstruction (17,20,21), and other applications. Basically, the unwanted background phase of an image is estimated from the image itself through either low-pass filtering (17,20) or parameter fitting with a low-order model (22–25). After this background phase is estimated, the image can be phase corrected to facilitate additional processing.

The new PC technique we propose, henceforth referred to as nonsubtractive PC velocity imaging, also is based on this assumption of slow background phase variation. Only a single (flow-encoded) image is acquired. The undesirable background phase of this image is estimated through a combination of low-order model fitting and low-pass filtering of the image. After this estimated background phase is removed from the image, the remaining phase is presumed to be coming from the flow-encode alone, and a PC velocity image is formed. This method can be extended to the measurement of flow in more than one direction, although in such cases, the time saved would be less than 50%.

From the above description, it is clear that we distinguish between the flow-induced phase and the background phase on the basis of their differing spatial frequency. We assume that the flow we want to investigate is confined in some structure of primarily high spatial frequency content, such as blood vessels. The background phase, however, is assumed to vary much more slowly. Therefore, our low-order modeling plus low-pass filtering predominantly captures only the background phase and rejects the phase from flow. Of course, this phase estimation step can never be perfect, and a certain amount of error has to be tolerated. In the next section, we describe some ways to minimize this error.

Improving Image Quality and Measurement Accuracy

As discussed earlier, the image quality and velocity measurement accuracy depend primarily on how well we can separate the flow phase from the background phase. To this end, two lines of improvement are available. First, we can improve our algorithm for background phase estimation. Second, we can suppress relatively fast variations in the background phase by carefully designing the imaging sequence so that it becomes more easily separable from the flow phase. These two approaches will be discussed in order.

Existing methods for background phase estimation either do a direct linear low-pass filtering of the image followed by phase extraction, or a low-order (polynomial) model is fit to the image phase. These methods work well for their applications because the background phase indeed contains a very low spatial frequency content (typically for spin-echo images) and because phase correction errors tend to produce a relatively harmless mild blurring in the real channel, which is the output channel they used. In our application, however, the situation is less favorable. First, flow imaging in general does not use spin-echo sequences. Without the benefit of spin echoes that suppress off-resonance dephasing, the background phase of flow images usually exhibits greater variations as a result of inhomogeneity and susceptibility effects. Second, for PC velocity imaging, errors in the phase correction do not get attenuated in the final velocity image, as they would be if one only displayed the real channel. Instead, they manifest as significant image artifacts and velocity measurement errors. Because of these added difficulties, we find neither simple linear low-pass filtering nor low-order modeling adequate in estimating the background phase.

To overcome this problem, we propose the use of a low-order polynomial model in combination with 2D median low-pass filtering. By fitting the phase of the image to a 2D polynomial model, the global trend of the background phase variation is captured. After this global phase trend is removed, 2D median filtering is performed on the normalized (i.e., intensities of all pixels scaled to unit magnitude) real and imaginary parts of the image separately, and the phase of the resulting image is used in an additional phase correction to the unfiltered image. We chose the nonlinear median filter because of its well-known ability to cleanly remove spike noise and isolated lines and also for its general robustness. Because the flow phase from a highly confined vessel very much resembles a spike or an isolated line on a background of slowly varying phase, a median filter with a sufficiently large kernel can effectively remove it from the background phase estimate with little ''leakage.''

The second approach to improving image quality involves the use of short-echo-time imaging sequences. For an image acquired without a spin echo, the shorter the echo time, the less time there is for off-resonant phase to accrue and the lower the phase distribution's spatial frequency bandwidth will be. Because this phase induced by off-resonance is the main contributor to fast variations in the background phase, a short echo time is effective in reducing its overall spatial frequency bandwidth. As an additional benefit, short echo times also can reduce the extent of intravoxel dephasing in fast or irregular flow and hence will give a superior depiction of vessels in general.

Finally, in the case of time-resolved imaging of pulsatile blood flow through stationary structures (e.g., arteries), we recognize that the background phase should be the same in every time frame and as such can be separated from the time-varying phase due to flow. We simply set a threshold

to the velocity time variation below which the measured velocity is assigned to be 0. This procedure can be viewed as a step of temporal high-pass filtering. Note that this step will not improve the velocity measurement accuracy but is useful in enhancing the overall image quality through suppressing the stationary background.

Practical Implementation

With the above considerations in mind, we implemented a short-echo-time interleaved spiral imaging sequence to test our nonsubtractive technique. The spiral was chosen because of its good flow property, high speed, and short echo time. When the acquisition was 3D, a cylindrical stack-of-spirals trajectory was used (26). All spiral readouts were 14.4 msec long in our implementation. As for the RF excitation, we have decided to use a 16-msec minimum-phase fat saturation pulse followed by a truncated-sinc excitation rather than a single spectral-spatial pulse because the former allows a much shorter echo time (Fig. 1). (The spikes at the beginning and the end of the fat saturation pulse are a result of optimization through the Shinnar–Le Roux algorithm (27).) Between the RF and the readout, either a flow-encoding or a flow-compensation gradient was inserted (the latter was used to obtain the reference image in conventional PC velocity imaging, which we performed for comparison). They were combined with the refocusing lobe of the truncated-sinc excitation to shorten the echo time. This combination of fat-suppressed excitation and flow encoding allowed us to achieve echo times as short as 3–4 msec on standard hardware (22 mT/m maximum gradient strength, 20 mT/m/msec slew rate limit), depending on the value of v_M and the slice thickness. All experiments were carried out on a GE 1.5-T Signa Scanner.

After acquisition, the spiral data was reconstructed by using a gridding algorithm (28). A conventional PC image was generated as the standard for comparison. Residual velocity errors due to eddy current effects were corrected for by fitting a second-order polynomial to the velocity measured at regions known to be stationary and then subtracting this polynomial fit from the velocity image (11). This method worked well for most parts of the body. For the coronary imaging experiment described later, there was not sufficient stationary material surrounding the vessel of interest, so we corrected for eddy current effects by using the method of phantom calibration described by Keegan et al. (13).

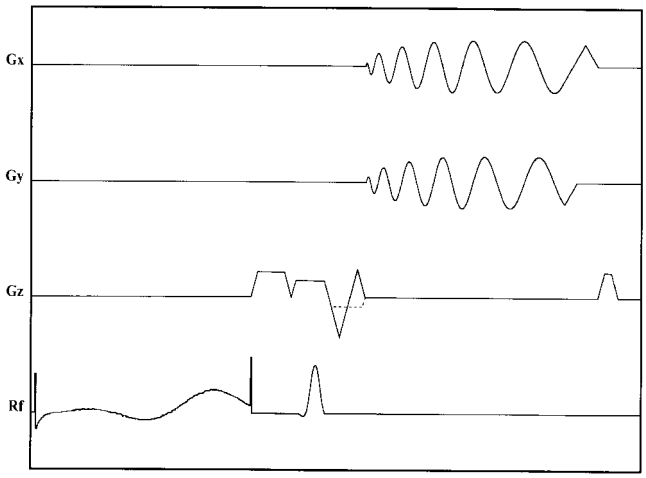

FIG. 1. The pulse sequence used. In G_z (slice-select), the solid line and the broken line represent the flow-compensated and the flow-encoding waveforms, respectively.

To generate the nonsubtractive PC image, we took the flow-encoded image and fitted a fourth-order 2D polynomial to its real and imaginary parts separately at areas of sufficient SNR. The phase of the resultant fourth-order complex polynomial was removed from the image, and a 2D median filter was applied to the normalized real and imaginary parts of the resultant image separately. The kernel size of the filter was chosen to be roughly double the diameter of the largest vessel that we wanted to measure. This represented a compromise between noise immunity and the ability to track relatively rapid background phase variations. However, we found that the results we obtained were quite insensitive to the size of the filter kernel (e.g., when it varies from 1.7 to 3 times the largest vessel size). This is an added advantage over linear filters such as the Fourier low-pass filter (i.e., convolution with a sinc kernel), which tend either to be inadequate in tracking the background phase variations (when the filter bandwidth is too low) or to allow significant leakage from the high-frequency flow-induced phase into the background phase estimate (when bandwidth is too high). The median filter alleviated this problem considerably. After the phase of this median-filtered image was removed from the polynomial model phase-corrected image, we obtained the final phase-corrected image. Its phase was multiplied by v_M/π to give the nonsubtractive PC velocity image. No additional eddy current correction was necessary, because eddy current effects had implicitly been corrected through the use of the polynomial model.

In cases where a time-resolved data set was acquired over a stationary object containing pulsatile flow, this a priori information was exploited. First, instead of using a different background phase estimate for each time frame, we averaged all these estimates together to provide a single (more accurate) estimate and used it in all frames. The averaging was calculated according to the following formula:

$$\phi = \mathrm{Arg}\left(\sum_{n=1}^{N} e^{j\phi_n}\right) \qquad [2]$$

where ϕ_n is the phase estimate derived from the nth frame alone and ϕ is the averaged estimate. Second, after generating the time series of nonsubtractive PC images, we calculated the standard deviation of each pixel's velocity variation over time. Pixels with standard deviations smaller than the noise standard deviation were considered to be pixels of stationary material, and we assigned a velocity of 0 to them in our final velocity image. We refer to this step in our processing as ''stationary background rejection.''

RESULTS

Phantom Experiment

We validated the proposed nonsubtractive PC velocity imaging scheme on a phantom consisting of a 6.4-mm-ID

tubing filled with copper sulfate solution that flowed at a speed of up to 1 m/sec. A 1-cm-thick slice perpendicular to the flow was excited, and a v_M of 135 cm/sec was used for flow measurement. We also measured the flow rate separately by using the ''bucket and stopwatch'' technique. The results of the experiment are shown in Figure 2, where a 13 × 13 median filter kernel was used in the nonsubtractive technique, because the tube diameter was about 6 pixels wide. The average flow velocity calculated using our nonsubtractive PC technique agrees well both with conventional PC and with the bucket-and-stopwatch measurements; the average errors were ±1.7 cm/sec and ±2.5 cm/sec, respectively.

Abdominal Aorta

We tested the proposed nonsubtractive PC technique for its ability to image aortic blood flow. A 1-cm-thick axial slice of the abdomen was excited, and a v_M of 135 cm/sec was used in the experiment. The sequence was electrocardiogram gated, and 15 time frames of data (45 msec between frames/2.9 msec echo time) were acquired within each heartbeat to capture the phasic flow. The flip angle was 50°, and the resolution was 3.1 mm × 3.1 mm. The imaging was completed within one breath hold (12 heartbeats of flow encoding interleaved with 12 heartbeats of flow compensation, plus 4 extra heartbeats to achieve equilibrium). An 11 × 11 median filter was used in the nonsubtractive technique. The results are shown in Figure 3. In Fig. 3a, we show the magnitude image from the flow-encoded data set acquired immediately after the ECG R-wave. Figure 3b and c then show the conventional and the nonsubtractive PC images, respectively, at a representative time point (210 msec after ECG R-wave). The nonsubtractive technique produces images of quality close to that of the conventional technique.

To demonstrate the benefits of stationary background rejection, we show in Fig. 3d the result when this step is omitted. More susceptibility-induced artifacts appear in this image because our background phase estimate cannot capture very fast phase variations. Next, in Figure 4, we show the cross-sectional flow profiles across both the aorta and the vena cava at various time points. It is evident that the nonsubtractive technique produces flow profiles with an accuracy comparable to that of the conventional method. To demonstrate the importance of our nonlinear filtering approach to background phase estimation, we show in Figure 5 the flow profiles obtained when the median filtering (and polynomial modeling) is replaced with a simple Hamming-windowed truncation in k-space. Stationary background rejection is omitted to illustrate the effects of the different filters on the background. The velocity measurement accuracy is considerably reduced (especially in the vena cava), and background artifacts are more severe, depending on the bandwidth of the truncation. Finally, in Figure 6, we plot the maximum flow velocity in the aorta (average of 4 central pixels) during the cardiac cycle as measured by both PC imaging methods. The time variation of aortic flow calculated from the nonsubtractive PC technique agrees well with that of the conventional PC technique; the systolic peak and early diastolic retrograde flow are well-depicted. The average discrepancy in velocity measurements between the two techniques is only ±2.6 cm/sec.

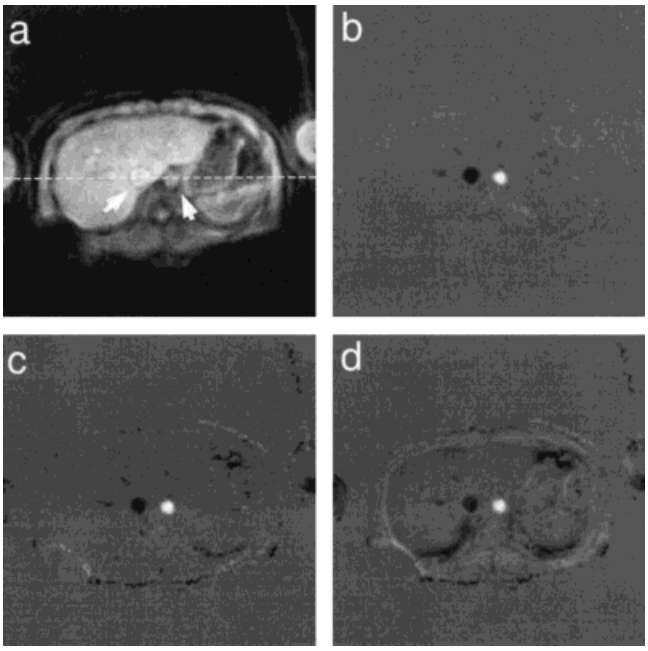

FIG. 3. Aorta phase contrast images. **a:** Magnitude image. **b:** Conventional PC image. **c:** Nonsubtractive PC image. **d:** Nonsubtractive PC image without stationary background rejection. Left and right arrows in a point to the vena cava and the aorta, respectively. Both **b** and **c** have stationary background rejection.

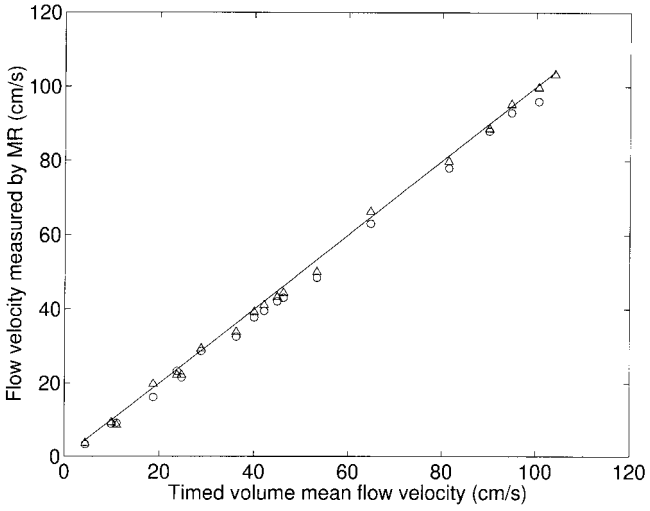

FIG. 2. Phantom flow velocity measurements. The straight line is the ''bucket and stop watch'' reference; triangles and circles are data points from conventional and nonsubtractive PC techniques, respectively.

Femoral Artery

We also have tested our method on the femoral artery, using the same imaging sequence as the one used to acquire our phantom and aorta images. To demonstrate that nonsubtractive PC velocity imaging can give a high-quality image when susceptibility effects are not significant, even if time-resolved information is not available, we did not perform stationary background rejection on the data. The

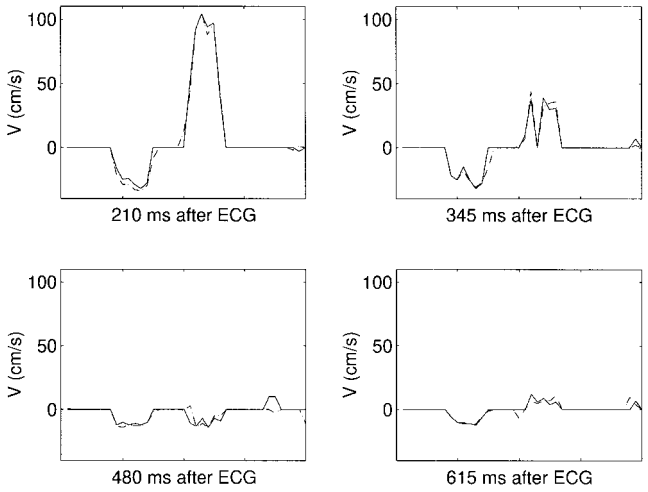

FIG. 4. Cross-sectional flow profile of aorta and vena cava. Cross-section is taken along the broken line in Fig. 3a. Only a small area surrounding the two vessels of interest is shown. In each graph, aorta is on the right and vena cava on the left.

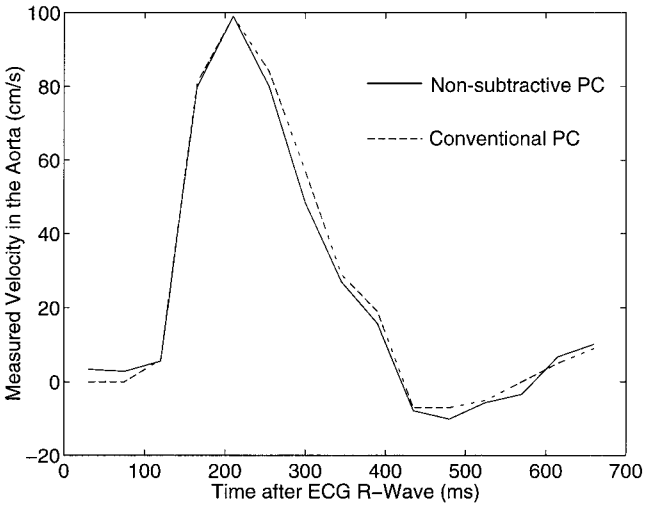

FIG. 6. Time variation of aortic flow velocity at the center of a lumen.

results are shown in Figure 7 for a representative time frame (345 msec after ECG trigger). Again, the nonsubtractive method gives a PC velocity image close to that of the conventional method. When the periodic time variation of maximum flow velocity is measured (2 central pixels were used for average), we find the average discrepancy between conventional and nonsubtractive PC imaging techniques is only ± 1.7 cm/sec (Fig. 8).

Carotid Arteries

To investigate the potential use of nonsubtractive PC velocity imaging in a case of significant clinical importance, we applied the technique to the 3D imaging of the carotid arteries. A 8-cm-thick axial slab of the neck and lower head of a healthy volunteer containing the carotid bifurcation was imaged by using a stack-of-spirals trajectory containing 16 planes of 12-interleaf spirals. The echo time and flip angle were 2.8 msec and 45°, respectively. We acquired 15 frames of data per heartbeat of the ECG gated scan, with an inter-frame time of 45 msec. The FOV was 20 cm $\times$ 20 cm $\times$ 10 cm and the image size was 128 $\times$ 128 $\times$ 16, acquired in 384 heartbeats with flow-encoded and flow-compensated acquisitions interleaved across heartbeats. A flow-encode gradient with v_M = 120 cm/sec was applied in the axial direction. Stationary background rejection was used to provide a cleaner looking nonsubtractive PC image (median filter kernel size 15 $\times$ 15). Figure 9 shows the resulting images at a representative time frame (120 ms after the ECG trigger) for two axial planes, the first 2 cm below and the second 4 cm above the bifurcation. At these two levels, the common carotid artery (CCA) and the internal carotid artery (ICA) are essentially perpendicular to the axial plane; hence, the flow velocity we measured should be very close to the absolute flow velocity inside the vessels. We see from these images that the flow in both the CCA and the ICA are well-captured by the nonsubtractive method. In Figure 10, the time variations of the maximum flow velocity in the CCA, ICA, and the external carotid artery (ECA) are shown. Both the conventional and the nonsubtractive method depict the characteristic flow patterns in these vessels clearly for a healthy subject. For example, in the CCA (Fig. 10a), we see a double peak (A, B) in systole, a sharp minimum (C) after end of systole, a flat wave in early diastole (D), and a minimum at end of systole (E) (29,30). Equally evident are the low pulsatility features of the flow (broad systolic peak, ample forward flow throughout diastole) in both the CCA and ICA (Fig. 10b). In contrast, the ECA in Fig. 10c displays the expected high-pulsatility features, such as the narrow sharp systolic peak and little flow in diastole, both clearly demonstrated by both methods. The average error of the nonsubtractive versus the conventional PC method is calculated to be ± 6, ± 2, and ± 6 cm/sec for the CCA, ICA, and ECA, respectively, in this example.

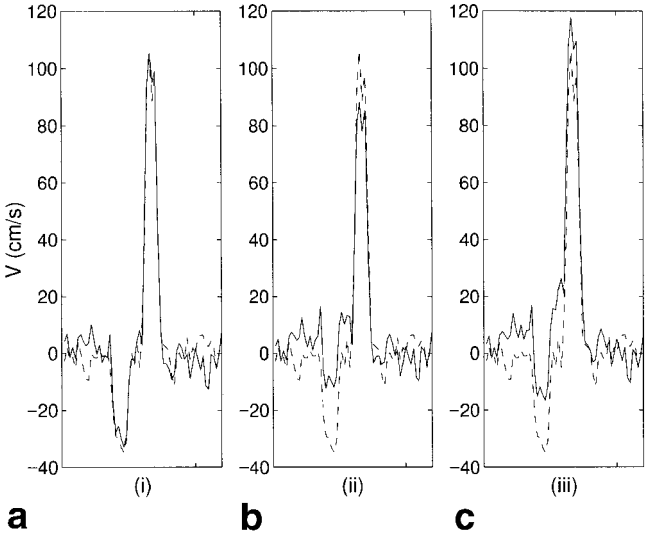

FIG. 5. Effects of different background phase estimation schemes on the aortic cross-sectional flow profile (at 210 msec after electrocardiogram R-wave). **a:** Low-pass filtering with polynomial model and median filter. **b,c:** Low-pass filtering with Hamming-windowed k-space truncation (truncate at one-fourth and one-eighth of maximum k-space extent, respectively). In all three graphs, the solid line is the result from the nonsubtractive PC technique, and the broken line is from the conventional PC technique.

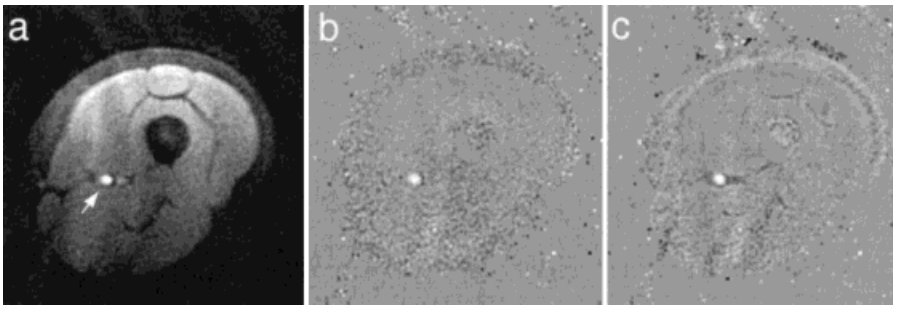

FIG. 7. Femoral artery PC images. **a:** Magnitude image. **b:** Conventional PC image. **c:** Nonsubtractive PC image. Arrow in a points to the femoral artery.

Coronary Arteries

We also have applied our method to the imaging of coronary blood flow as a preliminary assessment of its use in this highly challenging scenario. A 5-mm-thick axial slice of the heart of a healthy volunteer was imaged within a breath hold by using a surface coil to capture the proximal portion of the left anterior descending (LAD) coronary artery in plane. The bipolar gradient was applied in the left–right direction to look for flow coming out of the aorta into the coronary artery. A small v_M of 40 cm/sec was used, because we anticipated slow flow. Echo time was 4.3 msec, and the flip angle was 45°. The scan was plethysmograph gated, and we acquired 14 time frames per heartbeat with an inter-frame time of 45 msec. The image size was 128×128 over an FOV of 20 cm $\times$ 20 cm acquired with a 12-interleaf spiral. The results are shown in Figure 11, where a 9×9 median filter was used for the nonsubtractive method (stationary background rejection was not applicable, because the heart moves). Three consecutive time frames acquired at 100, 145, and 190 msec after the plethysmograph trigger (i.e., in early diastole) are shown. At other time points, the LAD was largely out of plane.

We see from a comparison of the magnitude images that flow encoding introduces substantial image artifacts. They result from beat-to-beat variations of the intracardiac blood flow, which give rise to data phase inconsistencies from interleaf to interleaf (13,31). More severe artifacts are produced when the flow sensitivity is high. Nevertheless, a comparison of the conventional and nonsubtractive PC velocity images shows that both depict the coronary flow quite well, although the latter is derived solely from the flow-encoded image with significant artifacts. One conspicuous difference, however, is that in the nonsubtractive velocity PC images, much of the blood flow in the heart chamber is suppressed because a substantial part of the broadly varying phase is taken as background in the phase estimation step and subsequently removed from the final images.

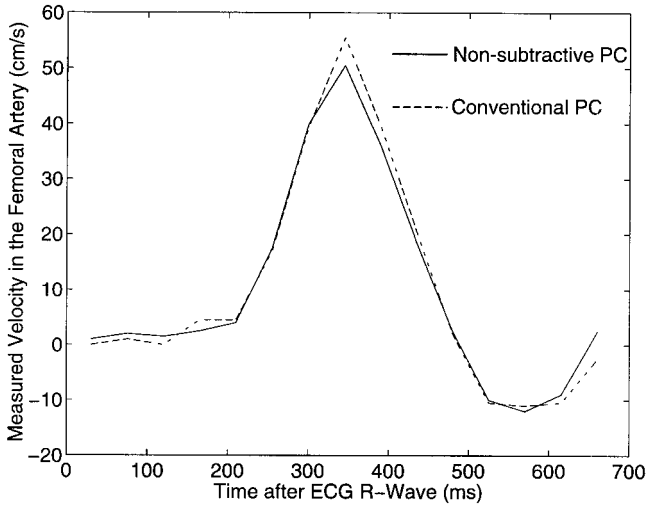

FIG. 8. Time variation of femoral artery flow velocity at the center of a lumen.

DISCUSSION

From the results presented earlier, we see that nonsubtractive PC velocity imaging is quite feasible in a variety of scenarios. The phantom experiment confirms that velocity measurements done by using the nonsubtractive technique are in good agreement with both conventional PC imaging and the more direct bucket-and-stopwatch approach, although our new technique tends to underestimate the velocities slightly. We attribute this to a small leakage of the flow phase into the background phase estimate. We believe, however, that this discrepancy of a few centimeters per second should be tolerable for most physiological applications.

In the aorta experiment, we demonstrated the feasibility and accuracy of the new technique in vivo. The flow in both the aorta and in the vena cava at all parts of the cardiac cycle are well-captured. Cross-sectional flow profiles are in excellent agreement with the conventional PC method. The time variation of the maximum aortic flow velocity measured follows the well-known tri-modal waveform. With the encouraging results shown in the present study, we expect that nonsubtractive PC velocity imaging can potentially be used to measure aortic flow in more clinically relevant scenarios (32,33). An additional possible improvement will be the use of variable v_M to increase measurement accuracy during the part of the cardiac cycle when slow flow is expected.

Similarly, the femoral artery example demonstrates the accuracy of the flow measurements and also confirms that without using temporal information to enable stationary background rejection, nonsubtractive PC velocity imaging still can produce flow images with few artifacts when the region of interest does not have substantial off-resonance shifts.

One example with possibly more immediate clinical relevance is the experiment on the carotid arteries, where 3D PC imaging provides accurate velocity information in addition to a complete 3D flow image. Fürst et al. (34) demonstrated the good correlation between conventional

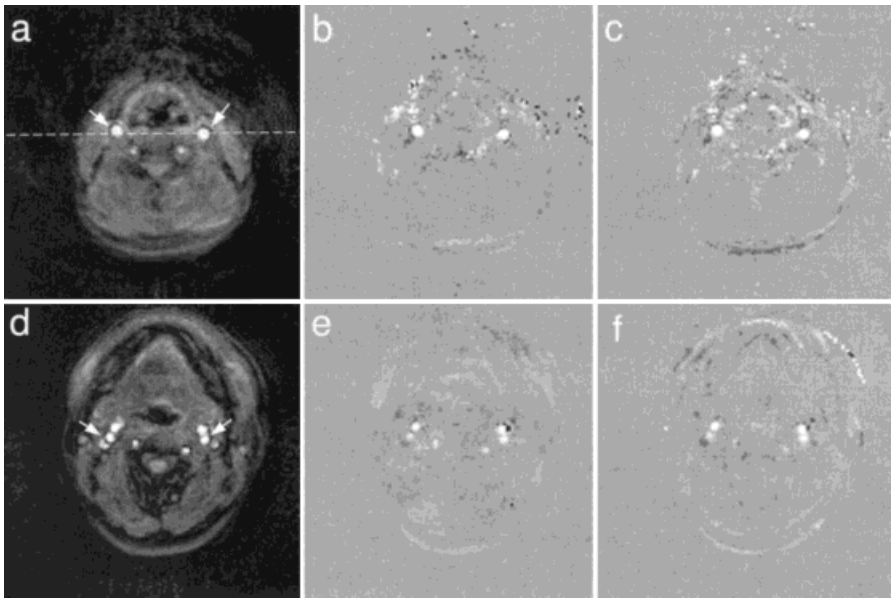

FIG. 9. Carotid artery PC images. Imaging plane is at 2 cm below and 4 cm above the carotid bifurcation for the top and the bottom row, respectively. **a:** Magnitude image. Arrows indicate the common carotid arteries. **b:** Conventional PC image. **c:** Nonsubtractive PC image. **d:** Magnitude image. Arrows indicate the internal carotid arteries. **e:** Conventional PC image. **f:** Nonsubtractive PC image.

PC techniques and ultrasound velocity measurements in the carotid arteries (the latter method being the the current gold standard), whereas Vanninen et al. (35) found that the peak systolic velocity at the post-stenotic ICA and and the volume flow rate ratio between the ICA and CCA are highly significant parameters in determining the stenotic grade. In our carotid experiment, we confirmed that velocity (and hence flow rate) values from nonsubtractive PC velocity imaging match those of conventional PC techniques very well in healthy subjects. Additional experiments are needed to confirm its use with carotid patients. If this use is established, nonsubtractive 3D PC velocity imaging may have an important application in assisting the grading of carotid stenosis. Because its scan time is shorter than that of conventional PC techniques, it reduces the risk of patient motion (e.g., swallowing) artifacts. Alternatively, we can trade off savings in scan time for increased resolution in the slab-select direction to produce an isotropic high-resolution 3D carotid image within a reasonable scan time. One more possibility is to tradeoff scan time reduction for an increased number of spiral interleaves. The readout time then could be shortened for reduced off-resonance sensitivity. We also envision that as faster gradients become available, the echo time can be shortened enough that flow at the stenosis can be imaged instead of leaving a signal void. Flow velocity at the stenosis then could be measured in MR just as in ultrasound, and nonsubtractive PC could become a fast method to provide both morphological and hemodynamic information at the stenosis.

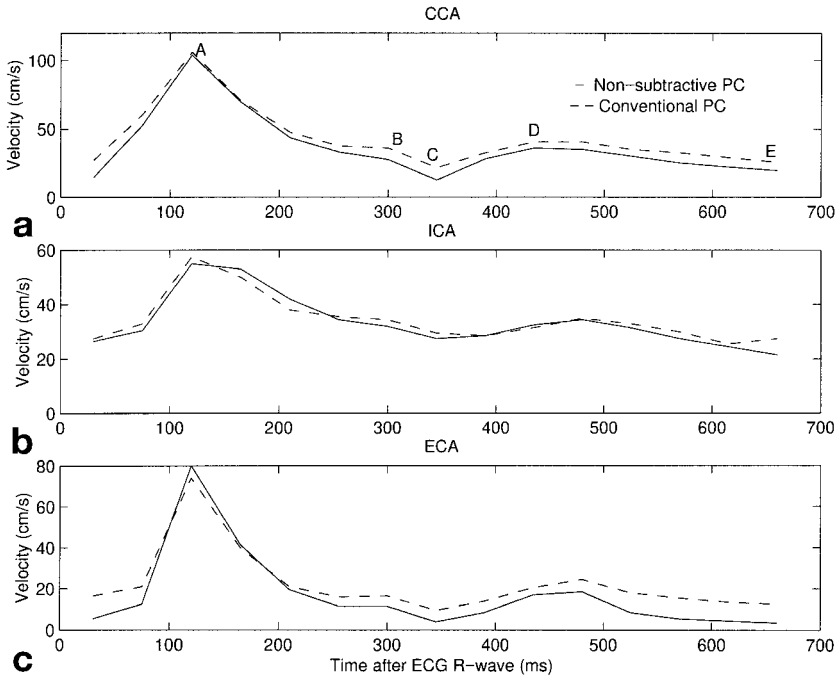

FIG. 10. Time variation of flow velocity measured at center of lumen in the left CAA (**a**), left ICA (**b**), and left ECA (**c**).

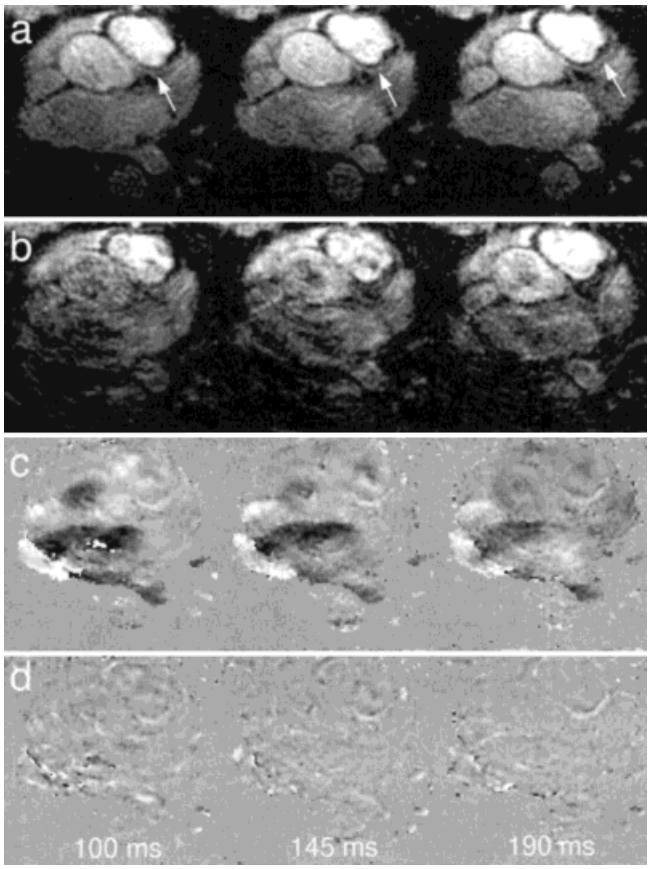

FIG. 11. PC images of the LAD. **a:** Magnitude image, flow compensated. **b:** Magnitude image, flow encoded at 40 cm/sec. **c:** Conventional PC image. **d:** Nonsubtractive PC image. Images in each row were obtained at 100, 145, and 190 msec, respectively, after the plethysmograph trigger. Arrows in **a** point to the LAD.

The last experimental example, imaging of the LAD, demonstrates the possibility of nonsubtractive PC velocity imaging in a rather non-ideal scenario. The coronary arteries, by virtue of their small size, slow flow, and significant bulk motion, present a significant challenge to flow imaging (13,36,37). As mentioned briefly earlier, one specific problem is that beat-to-beat variations in the heart chamber blood flow produce artifacts that limit the amount of flow sensitivity one can apply to the imaging sequence, thus greatly reducing the SNR of the PC velocity image. In the case of nonsubtractive PC velocity imaging, additional problems emerge, namely, that both susceptibility-induced magnetic field gradients and heart chamber blood motion tend to introduce errors into the background phase estimate. Fortunately, as our results have shown, with some care it is possible to obtain good coronary flow images with the nonsubtractive PC technique. In our example, there was little in-plane flow in the regions surrounding the LAD (i.e., the pulmonary artery, the aorta, and the left atrium) during early diastole; hence, the spurious phase due to background blood flow was small. The use of a short echo time imaging sequence was also very helpful in reducing susceptibility-induced phase.

Nevertheless, it is important to realize that the flow velocity measured with the nonsubtractive PC technique would not be very accurate in this case because of some erroneous phase contributions from the surrounding blood. Because of this limitation, together with the fact that a strong flow-encode generates a degraded anatomical image, we think that our technique will not replace conventional PC techniques for the purpose of coronary flow measurements but may be useful in a number of special situations. For example, in MR fluoroscopy (38,39) one may want to obtain flow direction information (e.g., to detect retrograde flow) without reducing the frame rate. Moreover, the phase subtraction of two images acquired at two different time points in the cardiac cycle can lead to blurring from vessel motion. Nonsubtractive PC velocity imaging can overcome both of these problems. Another conceivable application is the detection of fast jets of flow at regions of coronary stenosis. For this purpose, a large v_M could be used that gives at the same time a magnitude image with minimal artifacts and also an indication of the regions of fast flow along the vessel. The time saved from using the nonsubtractive technique then could be used to increase the image resolution for better visualization of the stenosis while keeping the acquisition to within, say, one breath hold.

Finally, we want to point out several possible drawbacks of the nonsubtractive PC technique. They include a slightly reduced accuracy in velocity measurement and increased artifacts in the velocity image, both due to errors in the background phase estimate. Possible sources of these are the leakage of the flow phase into the background phase, rapid local susceptibility changes, and imperfect fat suppression around the vessel of interest. Our experimental results have demonstrated that for arteries, this measurement error is usually within a few centimeters per second when v_M is around 1 m/sec. One should bear this in mind when considering whether to adopt the method for a particular application. In veins, which have an inherent susceptibility difference from the surrounding tissue because of their high deoxygenated blood content, there may be a higher measurement error. However, this susceptibility shift is usually <0.1 ppm (40), which translates to about 5 cm/sec with a 4-msec echo time and $v_M = 1$ m/sec. Depending on the actual oxygenation level of the venal blood and the angle between the vessel and the B_0 field, this error can be lower. When high-speed gradients are available, the echo time and, hence, the error due to susceptibility variations can be reduced. As for fat suppression, it can usually be done adequately within a small region around the vessel of interest when measuring through-plane flow. For in-plane flow, this may be more difficult and must be considered as a possible source of error. Depending on the application, however—particularly when the time-varying aspects of the flow is of main interest—this error appears as a constant bias and therefore should not pose a big problem. In general, the accuracy of nonsubtractive PC velocity imaging is higher for through-plane flow because a smaller 2D median filter (which can adapt to variations in the background phase more effectively) can be used.

A second drawback of nonsubtractive PC velocity imaging comes from the fact that the imaging sequence is never flow compensated. As a result, the available magnitude

image can contain more artifacts, especially when the flow is inconsistent. Another disadvantage stems from our basic assumption that the flowing material is mainly of high spatial frequency content. It implies that bulk flow such as that within the heart chambers cannot be captured. Finally, nonsubtractive PC velocity imaging also is not very applicable to situations in which the flow is primarily surrounded by air (e.g., in the thoracic aorta), because an accurate background phase estimate cannot be obtained at the vessel due to a lack of surrounding static tissue for phase reference.

CONCLUSIONS

We have demonstrated in many scenarios that nonsubtractive PC velocity imaging is an effective alternative to conventional PC velocity imaging, capable of a 50% scan time reduction when measuring flow in a single direction. With the use of a combination of short-echo-time acquisitions, better background phase estimation through nonlinear filtering, and the technique of stationary background rejection, flow images with quality and accuracy close to those from conventional PC velocity imaging can be obtained in the scan time normally required for the acquisition of a single image. We envision that the new technique could have major applications in highly time-constrained scenarios, such as 3D carotid imaging and breath-hold abdominal imaging.

ACKNOWLEDGMENTS

The authors thank Dan Thedens for help in the imaging sequence and Garry Gold for useful discussions.

REFERENCES

1. Moran PR. A flow velocity zeugmatographic interlace for NMR imaging in humans. Magn Reson Imaging 1982;1:197–209.
2. Pelc NJ, Herfkens RJ, Shimakawa A, Enzmann DR. Phase contrast cine magnetic resonance imaging. Magn Reson Quart 1991;7:229–254.
3. Ahn CB, Kim JH, Cho ZH. High-speed spiral-scan echo planar NMR imaging—I. IEEE Trans Med Imaging 1986;MI-5:2–7.
4. Meyer CH, Hu BS, Nishimura DG, Macovski A. Fast spiral coronary artery imaging. Magn Reson Med 1992;28:202–213.
5. Nishimura DG, Irarrazabal P, Meyer CH. A velocity k-space analysis of flow effects in echo-planar and spiral imaging. Magn Reson Med 1995;33:549–556.
6. Gatehouse PD, Firmin DN, Collins S, Longmore DB. Real time blood flow imaging by spiral scan phase velocity mapping. Magn Reson Med 1994;31:504–512.
7. Pike GB, Meyer CH, Brosnan TJ, Pelc NJ. Magnetic resonance velocity imaging using a fast spiral phase contrast sequence. Magn Reson Med 1994;32:476–483.
8. Weisskoff RM, Cohen MS, Rzedzian RR. Nonaxial whole-body instant imaging. Magn Reson Med 1993;29:796–803.
9. O'Donnell M. NMR blood flow imaging using multi-echo, phase contrast sequences. Med Phys 1985;12:59–64.
10. Axel L, Morton D. MR flow imaging by velocity compensated/uncompensated difference images. J Comput Assist Tomogr 1987;11:31–34.
11. den Kleef JJE, Groen JP. A spatially non-linear phase correction for MR angiography. In: Proceedings of the Fifth Annual Meeting of the Society of Magnetic Resonance in Medicine, Montreal, 1986. p 729.
12. Bernstein MA, Pelc NJ. Phase correction of complex-difference processed magnetic resonance angiograms. U.S. Patent 5226418, 1993.
13. Keegan J, Tuihof HH, Engels H, Nelson RC, Gerety BM, Chezmar JL, den Boer JA. ''Keyhole'' method for accelerating imaging of contrast agent uptake. J Magn Reson Imaging 1993;3:671–675.
14. Jhooti P, Gatehouse PD, Mohiaddin RH, Yang GZ, Firmin DN. MR velocity mapping using lower resolution reference images to reduce the acquisition time. In: Proceedings of the Joint Meeting of the Society of Magnetic Resonance and the European Society of Magnetic Resonance in Medicine and Biology, 1995, Nice, France. p 324.
15. Jhooti P, Gatehouse PD, Mohiaddin RH, Yang GZ, Firmin DN. MR velocity mapping using reduced sampling schemes to shorten the acquisition time. In: Proceedings of the Fourth Meeting of the International Society of Magnetic Resonance in Medicine, New York, 1996. p 1278.
16. Van Vaals J, Brummer ME, Dixon WT, Tuihof HH, Engels H, Nelson RC, Gerety BM, Chezmar JL, den Boer JA, ''Keyhole'' method for accelerating imaging of contrast agent uptake. J Mag Reson Imaging 1993;3:671–675.
17. Margosian P, Schmitt F, Purdy DE. Faster MR imaging: imaging with half the data. Health Care Instrum 1986;1:195–197.
18. MacFall JR, Pelc NJ, Vavrek RM. Correction of spatially dependent phase shifts for partial Fourier imaging. Magn Reson Imaging 1988;6:143–155.
19. Bernstein MA, Thomasson DM, Perman WH. Improved detectability in low signal-to-noise ratio magnetic resonance images by means of a phase-corrected real reconstruction. Med Phys 1989;16(5):813–817.
20. Noll DC, Nishimura DG, Macovski A. Homodyne detection in magnetic resonance imaging. IEEE Trans Med Imaging 1991;10:154–163.
21. McGibney GH, Smith MR, Nichols ST, Crawley A. Quantitative evaluation of several partial Fourier reconstruction algorithms used in MRI. Magn Reson Med 1993;30:51–59.
22. Bernstein MA, Perman WH. Least-squares algorithm for phasing MR images. In: Proceedings of the Sixth Annual Meeting of the Society of Magnetic Resonance in Medicine, New York, 1987. p 801.
23. Jermanowicz A, Hyde JS. Improved image formation algorithm for spin-warp imaging. In: Proceedings of the Ninth Annual Meeting of the Society of Magnetic Resonance in Medicine, New York, 1990. p 550.
24. McGibney GH, Smith MR, Nichols ST. Estimation of phase errors in magnetic resonance imaging. In: Proceedings of the Ninth Annual Meeting of the Society of Magnetic Resonance in Medicine, New York, 1990. p 563.
25. Hua J, Hurst GC. Noise and artifact comparison for Fourier and polynomial phase correction used with Fourier reconstruction of asymmetric data sets. J Magn Reson Imaging 1992;2:347–353.
26. Irarrazabal P, Nishimura DG. Fast three-dimensional magnetic resonance imaging. Magn Reson Med 1995;33:656–662.
27. Pauly J, Le Roux P, Nishimura D, Macovski A. Parameter relations for the Shinnar-Le Roux selective excitation pulse design algorithm. IEEE Trans Med Imaging 1991;10:53–65.
28. Jackson JI, Meyer CH, Nishimura DG, Macovski A. Selection of a convolution function for Fourier inversion using gridding. IEEE Trans Med Imaging 1991;10:473–478.
29. Baskett JJ, Beasley MG, Murphy GJ, Hyams DE, Gosling RG. Screening for carotid junction disease by spectral analysis of Doppler signals. Cardiovascular Res 1977;11:147–155.
30. Möller HE, Klocke HK, Bongartz GM, Peters PE. MR flow quantification using RACE: clinical application to the carotid arteries. J Magn Reson Imaging 1996;6:503–512.
31. Drangova M, Zhu Y, Pelc NJ. Effect of artifacts due to flowing blood on the reproducibility of phase-contrast measurements of myocardial motion. J Magn Reson Imaging 1997;7:664–668.
32. Chang JM, Friese K, Caputo GR, Kondo C, Higgins CB. MR measurement of blood flow in the true and false channel in chronic aortic dissection. J Comput Assist Tomogr 1991;15:418–423.
33. Mostbeck GH, Dulce MC, Caputo GR, Proctor E, Higgins CB. Flow pattern analysis in the abdominal aorta with velocity-encoded cine MR imaging. J Magn Reson Imaging 1993;3:671–623.
34. Fürst G, Sitzer M, Hofer M, Steinmetz H, Hackländer T, Müller E, Mödder U. Quantification of carotid blood flow velocity using MR phase mapping. J Comput Assist Tomogr 1994;18:688–696.

35. Vanninen RL, Manninen HI, Kaarina Partanen PL, Vainio PA, Soimakallio S. Carotid artery stenosis: clinical efficacy of MR phase-contrast flow quantification as an adjunct to MR angiography. Radiology 1995;194: 459–467.
36. Edelman RR, Manning WJ, Gervino E, Li W. Flow velocity quantification in human coronary arteries with fast, breath-hold MR angiography. J Magn Reson Imaging 1993;3:699–703.
37. Hofman MB, van Rossum AC, Sprenger M, Westerhof N. Assessment of flow in the right human coronary artery by magnetic resonance phase contrast velocity measurement: effects of cardiac and respiratory motion. Magn Reson Med 1996;35:521–531.
38. Riederer SJ, Tasciyan T, Farzaneh F, Lee JN, Wright RC, Herfkens RJ. MR fluoroscopy: technical feasibility. Magn Reson Med 1988;8: 1–15.
39. Kerr AB, Pauly JM, Hu BS, Li KC, Hardy CJ, Meyer CH, Macovski A, Nishimura DG. Real-time interactive MRI on a conventional scanner. Magn Reson Med 1997;38:355–367.
40. Lai S, Haacke EM, Reichenbach JR. In vivo quantification of brain activation-induced change in cerebral blood oxygen saturation using MRI. In: Proceedings of Fourth Annual Meeting of the International Society of Magnetic Resonance in Medicine, New York, 1996. p 1756.